Supplementary Materials

Discovering Virtual Na-based Argyrodites as Solid-State Electrolytes Using DFT, AIMD, and Machine Learning Techniques

Byung Do Lee[1, §], Deepak Subhash Gavali[1, §], Heejeong Kim[1], Seonghwan Kim[1], Min Young Cho[1], Kyunglim Pyo[1], Young-Kook Lee[2], Woon Bae Park[3,] and Kee-Sun Sohn[1,*]*

[1]Faculty of Nanotechnology & Advanced Materials Engineering, Sejong University, 209 Neungdong-ro, Gwangjin-gu, Seoul, 143-747, South Korea

[2]Department of Materials Science and Engineering, Yonsei University, Seoul, 03722, Republic of Korea.

[3]Department of Advanced Components and Materials Engineering, Sunchon National University, Chonnam 57922, South Korea

[§] These authors contributed equally

*Corresponding authors: kssohn@sejong.ac.kr, wbpark@scnu.ac.kr

Table of Contents

Supplementary Figures

Supplementary Tables

Supplementary References

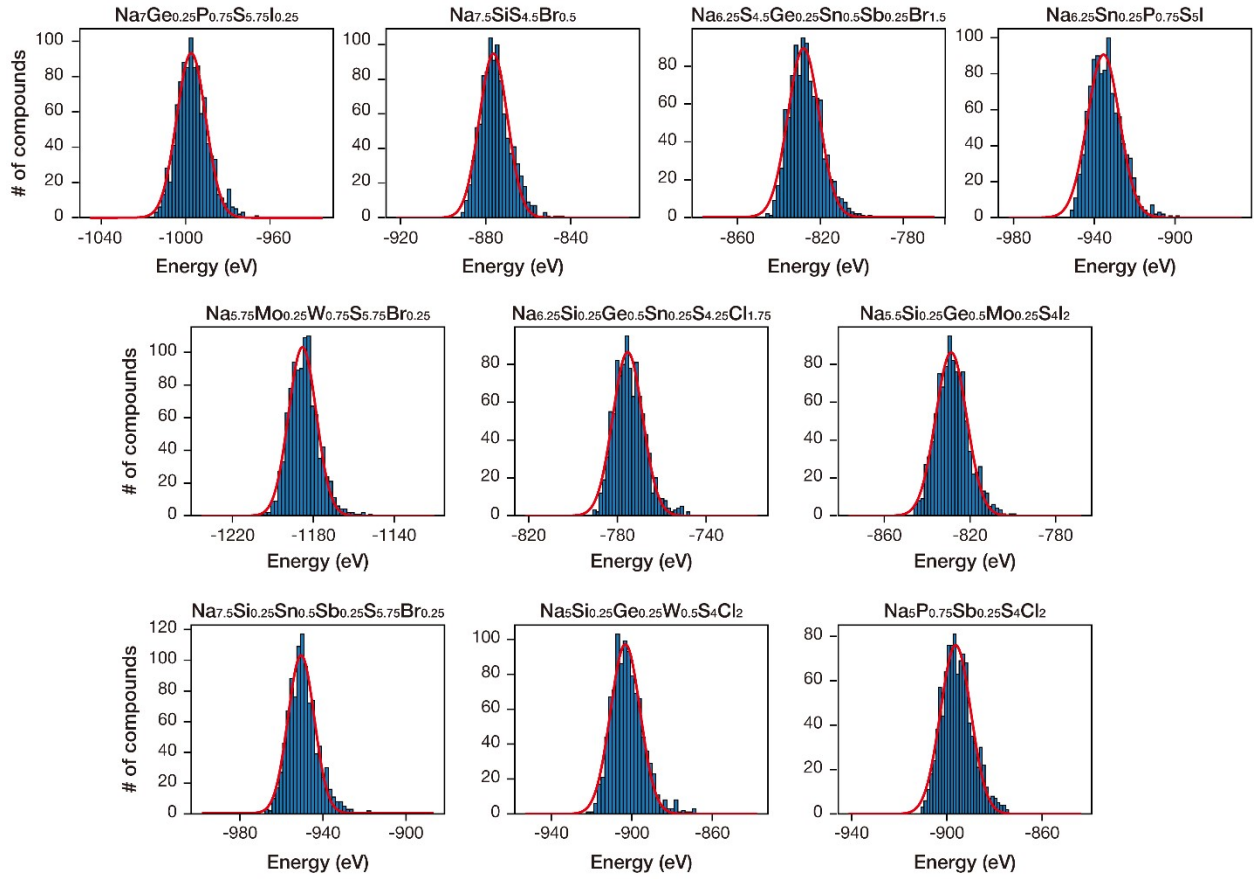

Fig. S1. Coulomb energy distribution over 1000 randomly selected configurations for each of 10 randomly selected Na-based argyrodite structures, exhibiting a typical Gaussian distribution. The Gaussian fit is shown as a red line.

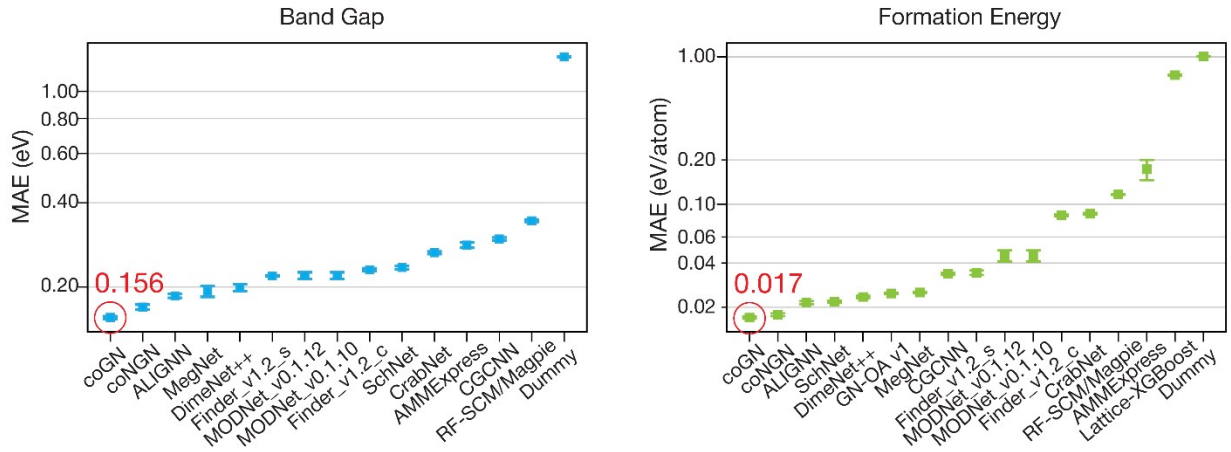

Fig. S2. Property (E_f and E_g) regression for inorganic crystals in the MP database, achieving state-of-the-art (SOTA) performance in benchmark tests[1]. coGN and coNGN mark the first and second lowest MAEs in comparison to many other ML models. a Displays the MAE for 16 different DL models in predicting formation energy (E_f), encompassing coGN[2], coNGN[2], ALIGNN[3], SchNet[4], DimeNet++[5], GN-OA v1[6], MegNet[7], CGCNN[8], Finder_v1.2_s[9], MODNet_v0.1.12[10], MODNet_v0.1.10[10], Finder_v1.2_c[9], CrabNet[11], RF-SCM/Magpie[1], AMMExpress[1] and Lattice-XGBoost[12]. b Illustrates the MAE of 14 DL models for band gap (E_g) prediction, including coGN[2], coNGN[2], ALIGNN[3], MegNet[7], DimeNet++[5], Finder_v1.2_s[9], MODNet_v0.1.12[10], MODNet_v0.1.10[10], Finder_v1.2_c[9], SchNet[4], CrabNet[11], AMMExpress[1], CGCNN[8] and RF-SCM/Magpie[1]. The 'Dummy' model serves as a baseline, providing random property evaluations to standardize the comparison framework[1]. The depicted MAE values are recalculated from the MatBench[1] as discussed in the main text of the manuscript.

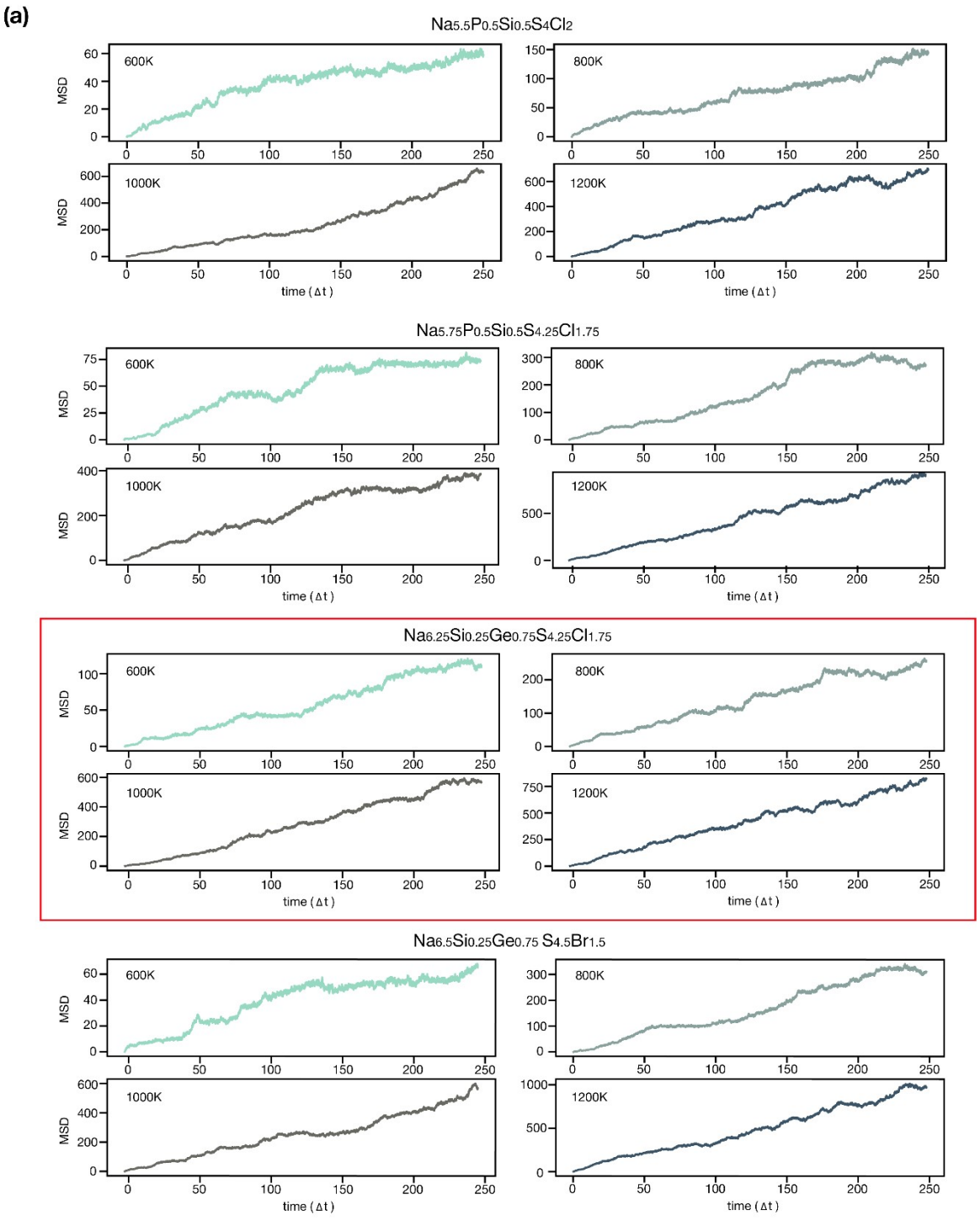

Fig. S3. Mean Square Distance (MSD) plots at all temperatures for these 15 entries. **(a)** Conventional total MSD method and **(b)** segmented MSD method. The five entries that were finally pinpointed are marked with red boxes.

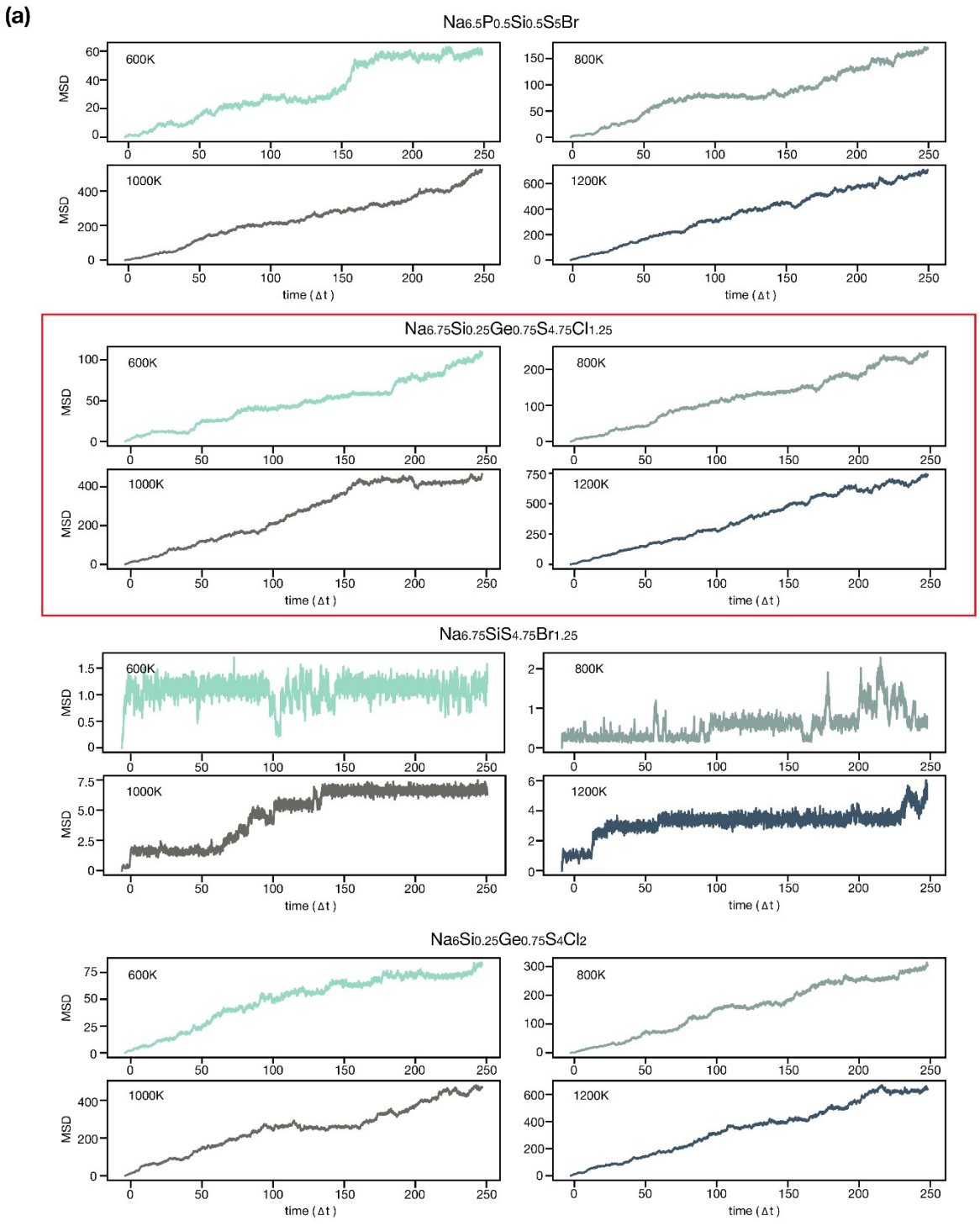

Fig. S3. (Continued)

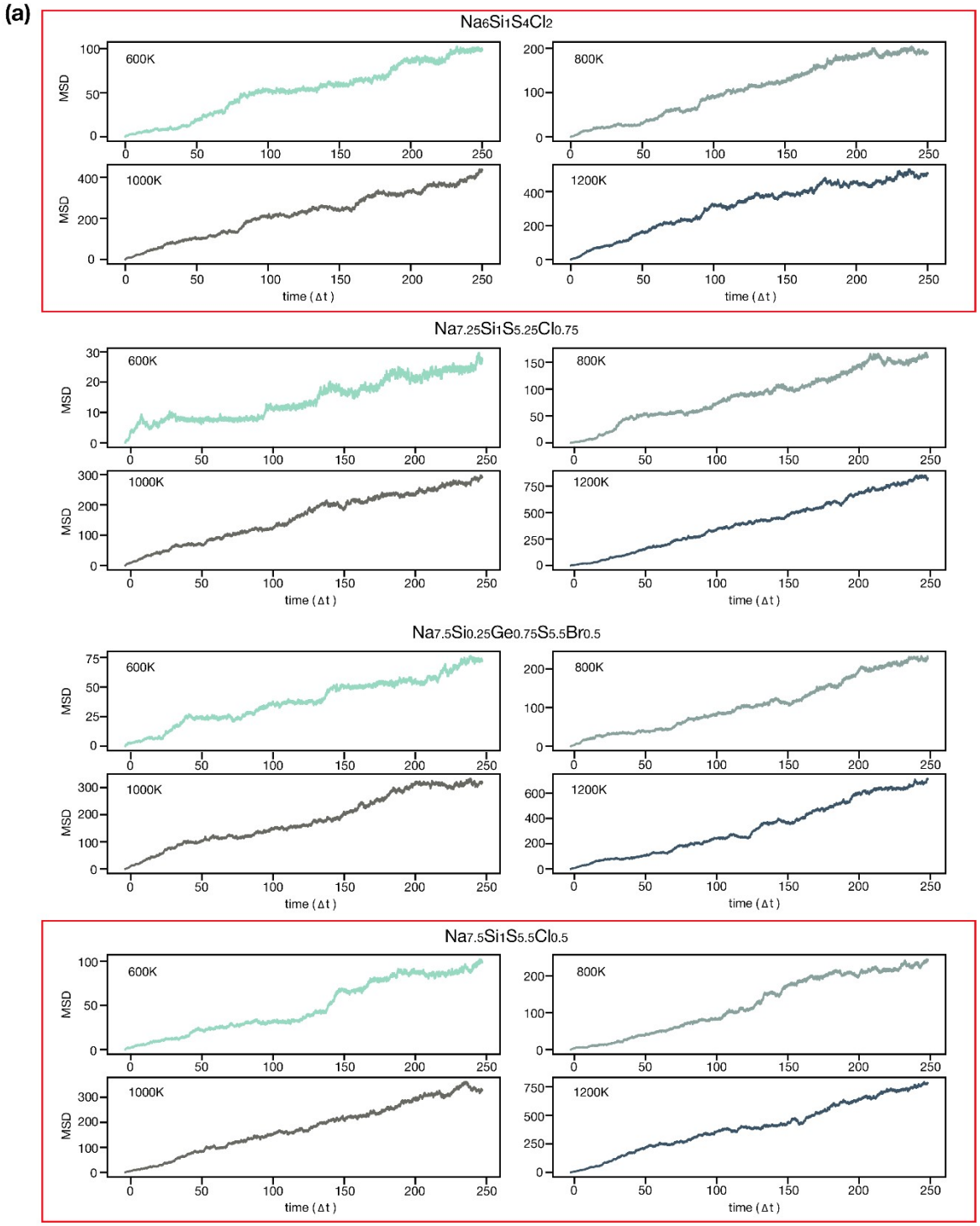

Fig. S3. (Continued)

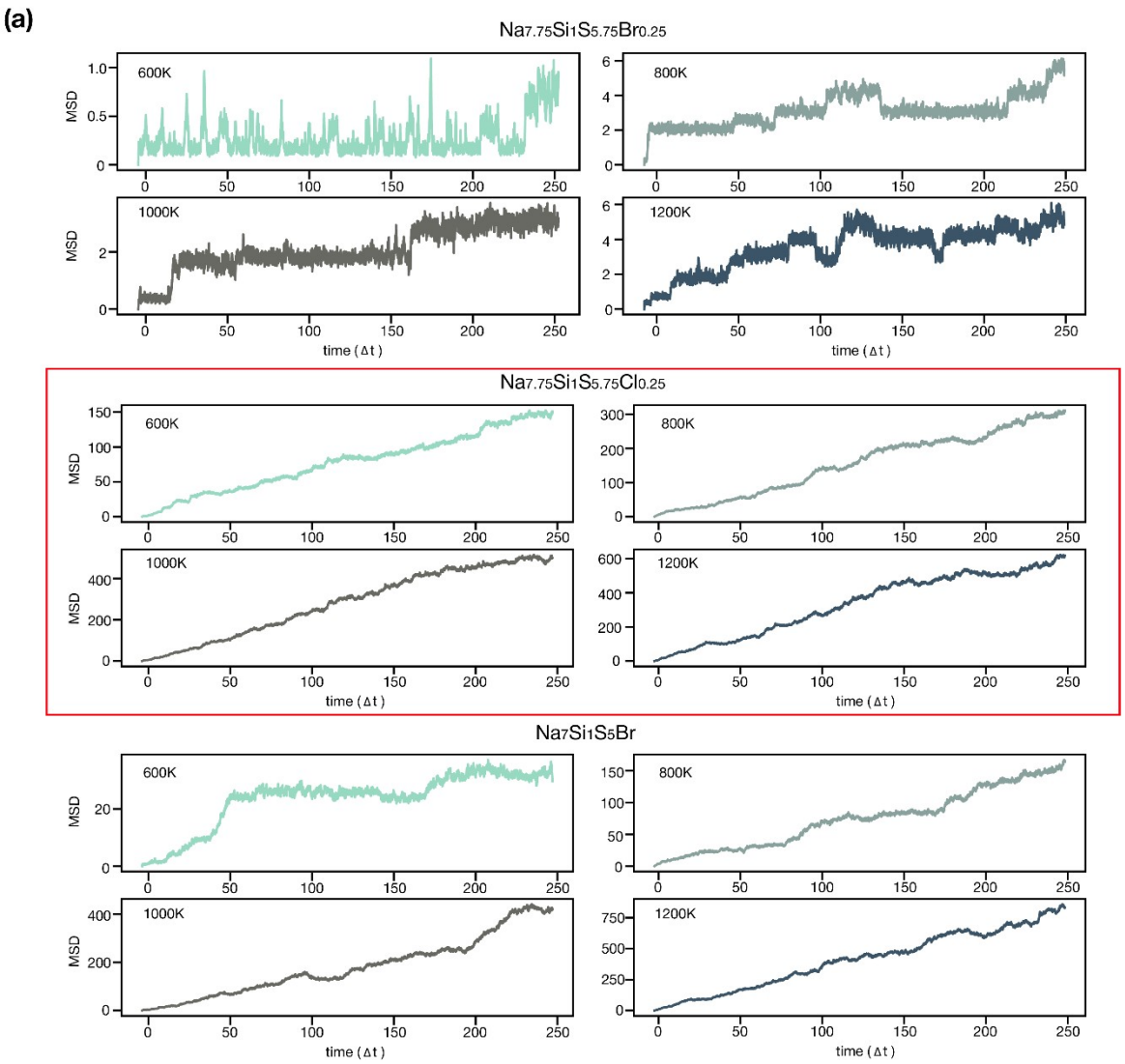

Fig. S3. (Continued)

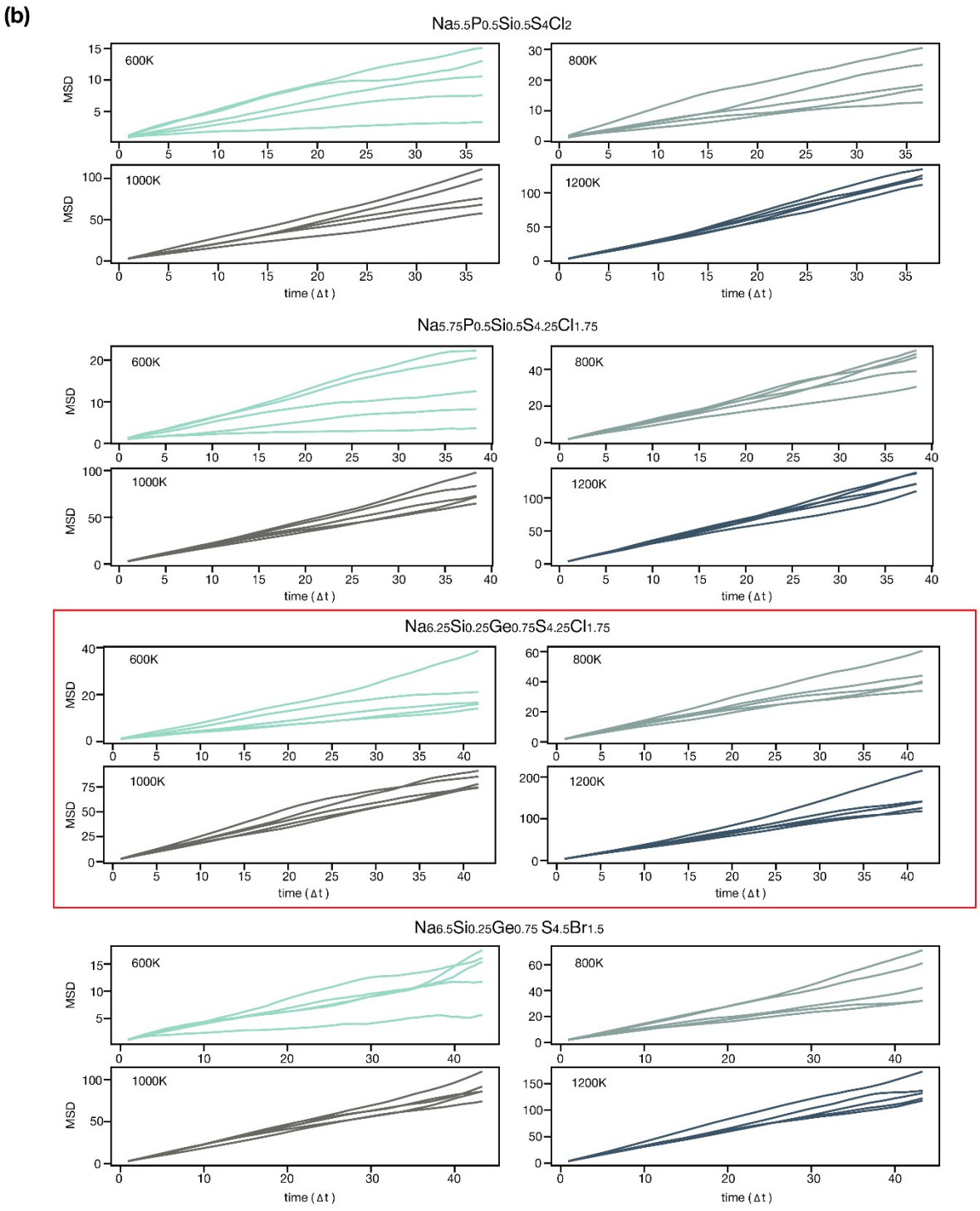

Fig. S3. (Continued)

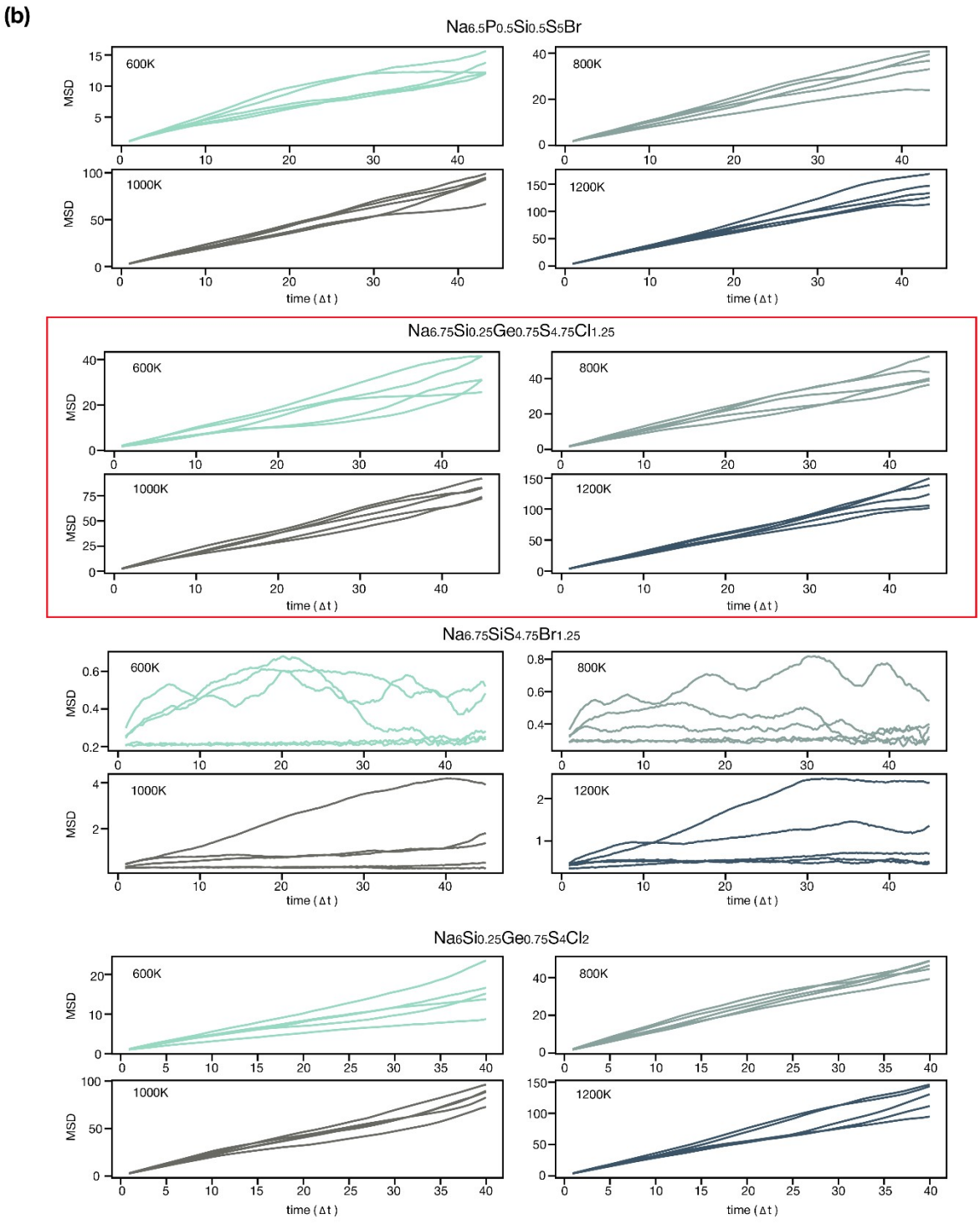

Fig. S3. (Continued)

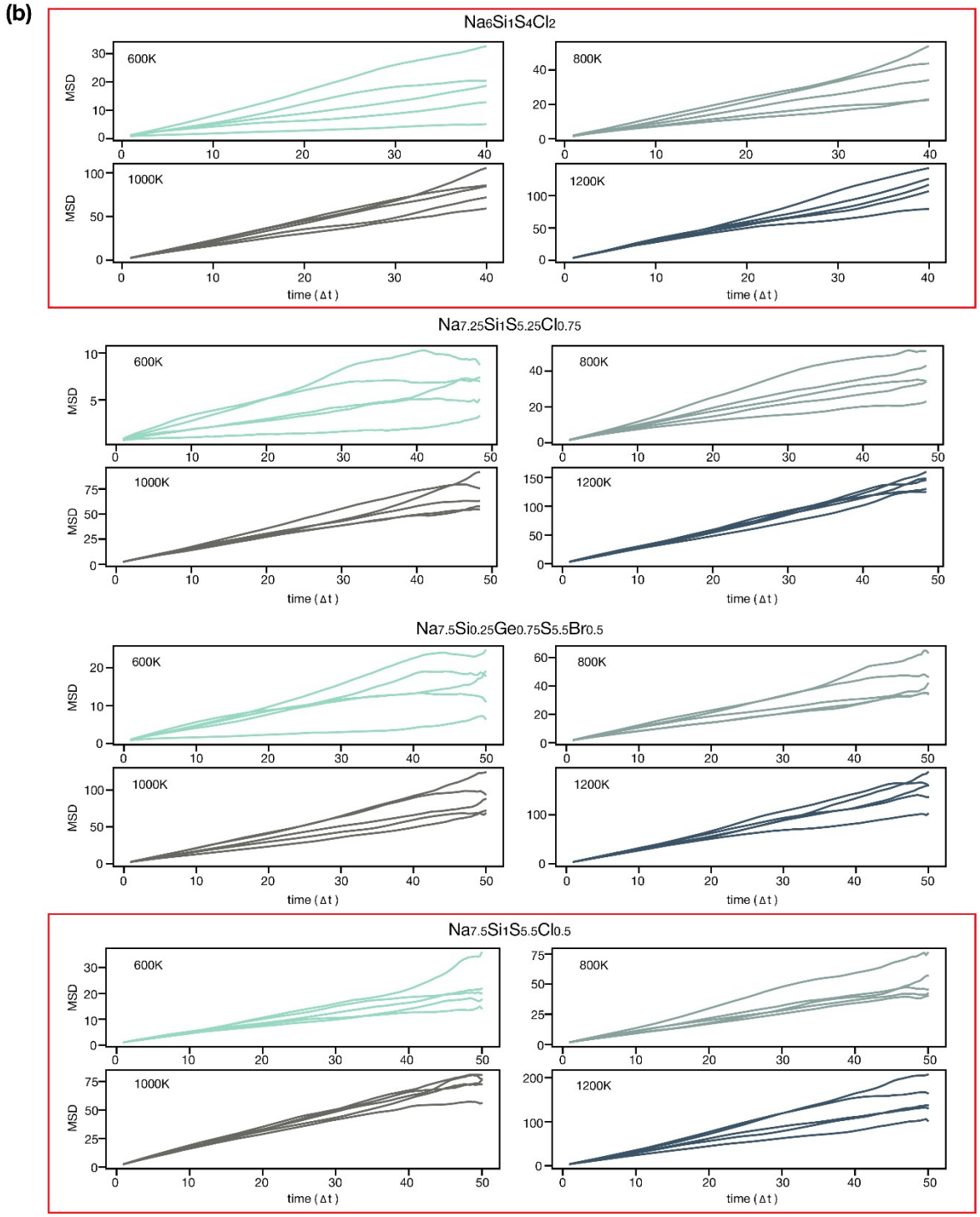

Fig. S3. (Continued)

(b)

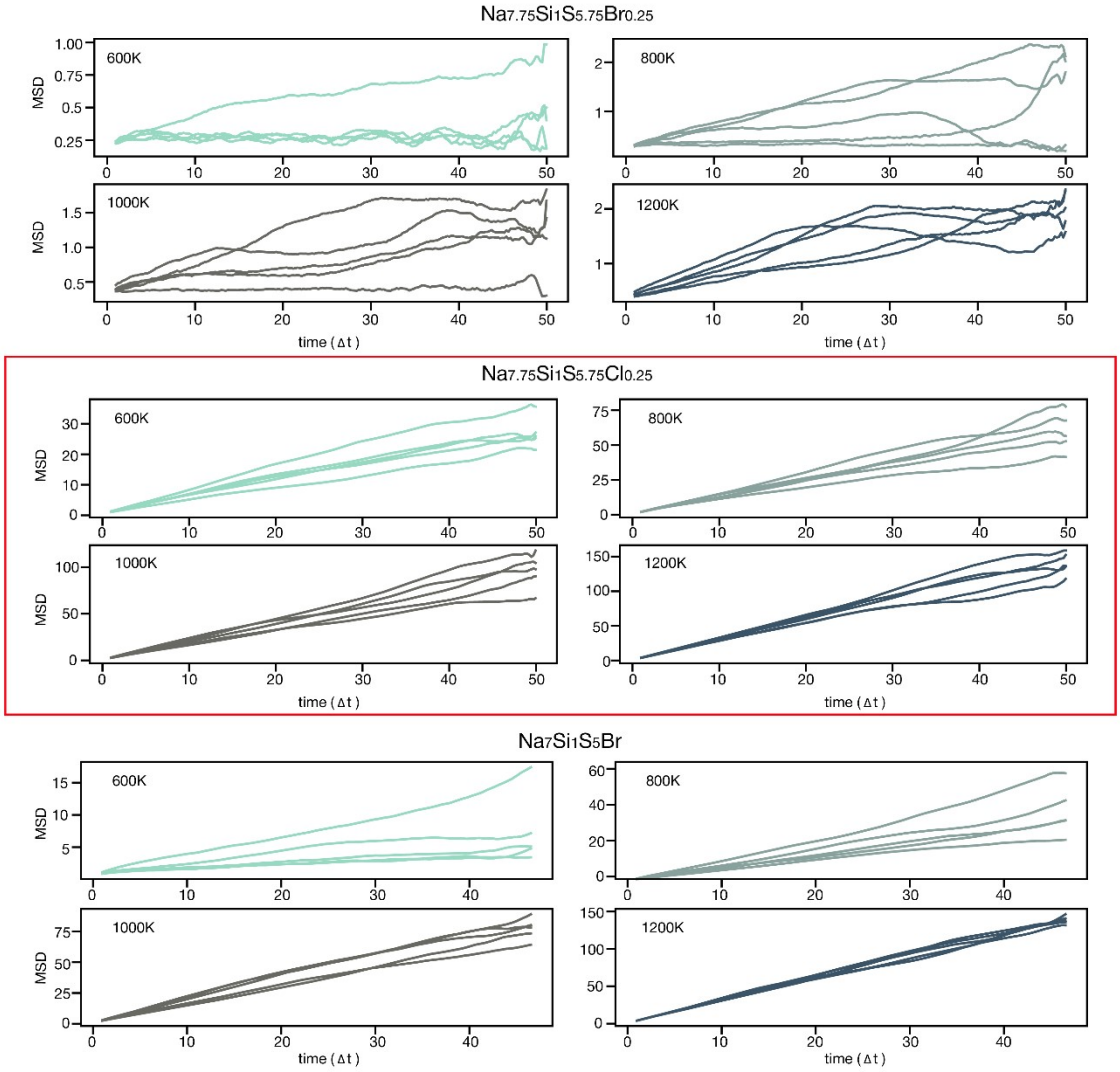

Fig. S3. (Continued)

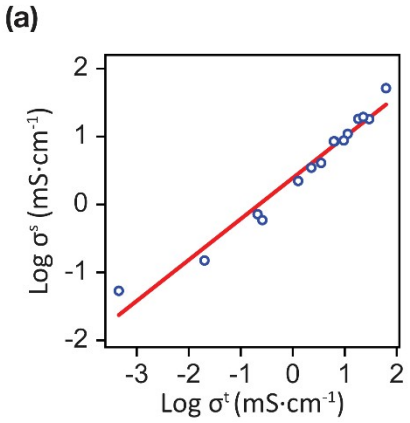

Fig. S4. (a) The plot of σ^{T}_{RT} vs σ^{S}_{RT}, exhibiting a clear linear relationship between σ^{T}_{RT} and σ^{S}_{RT}. **(b)** Arrhenius plots of the selected five candidates, showing σ^{T}_{RT} and σ^{S}_{RT}. The five entries that were finally pinpointed are marked with red boxes.

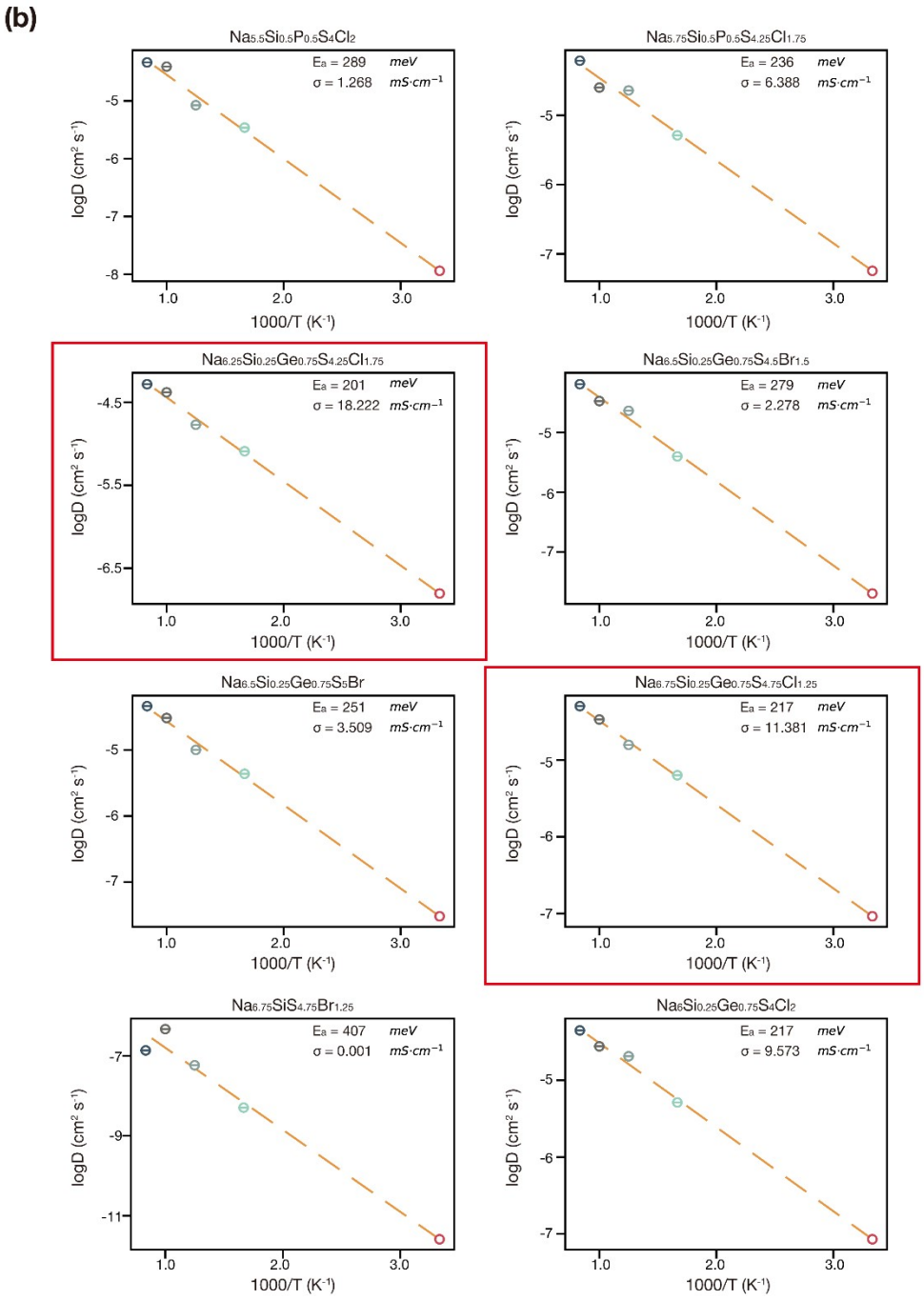

Fig. S4 (b). σ^{T}_{RT} results.

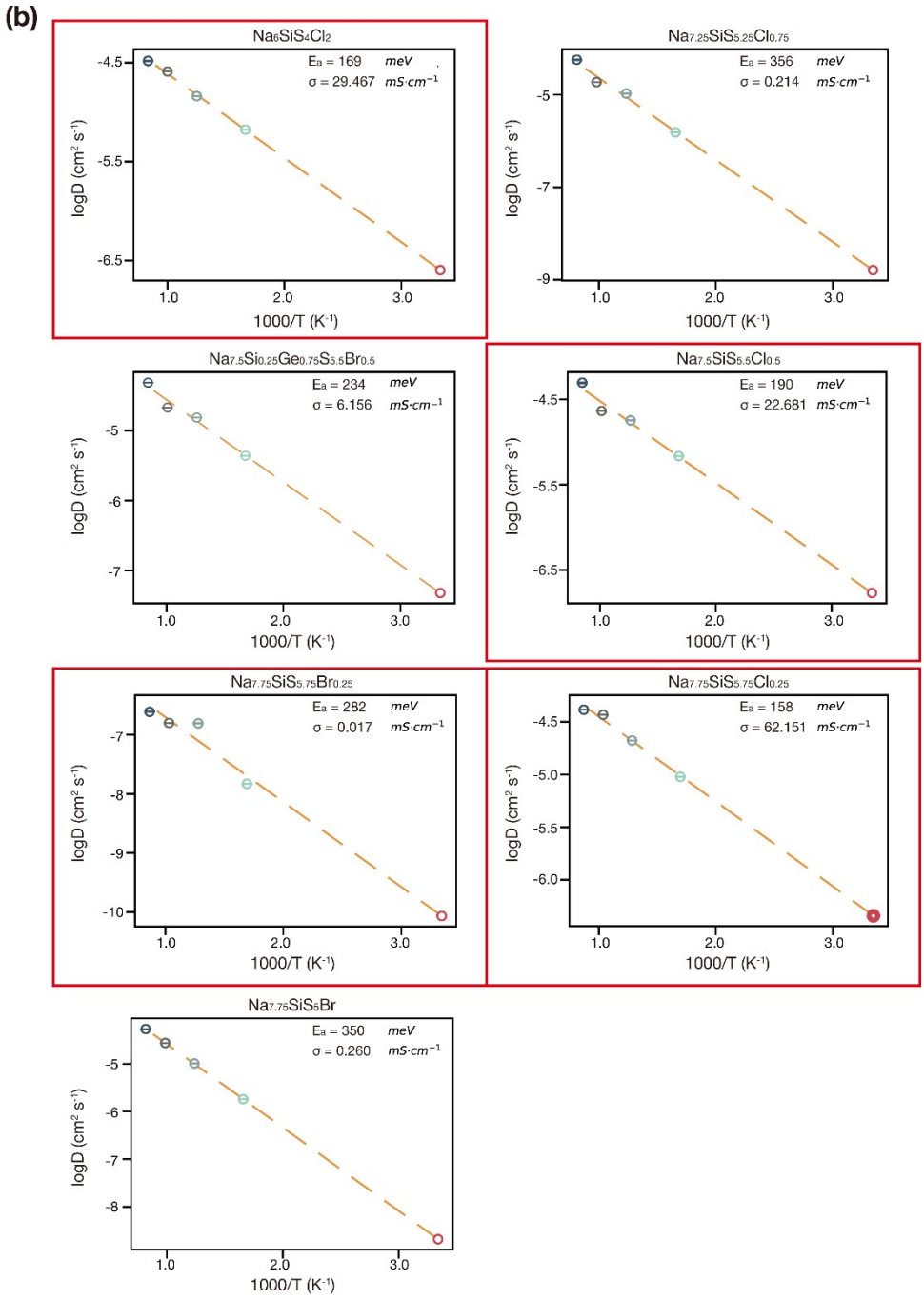

Fig. S4 (b). σ^{T}_{RT} results.

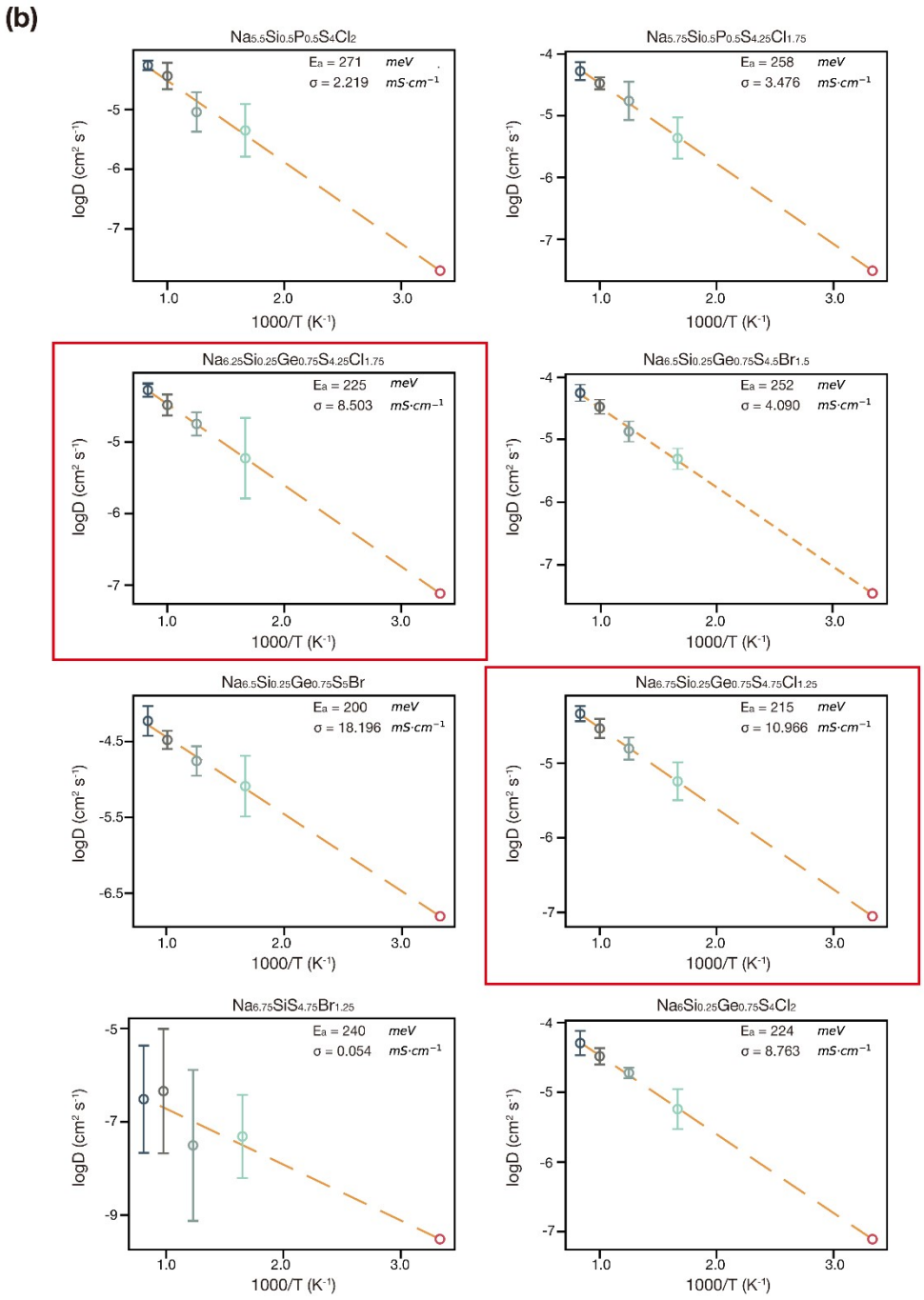

Fig. S4 (b). σ^{S}_{RT} results.

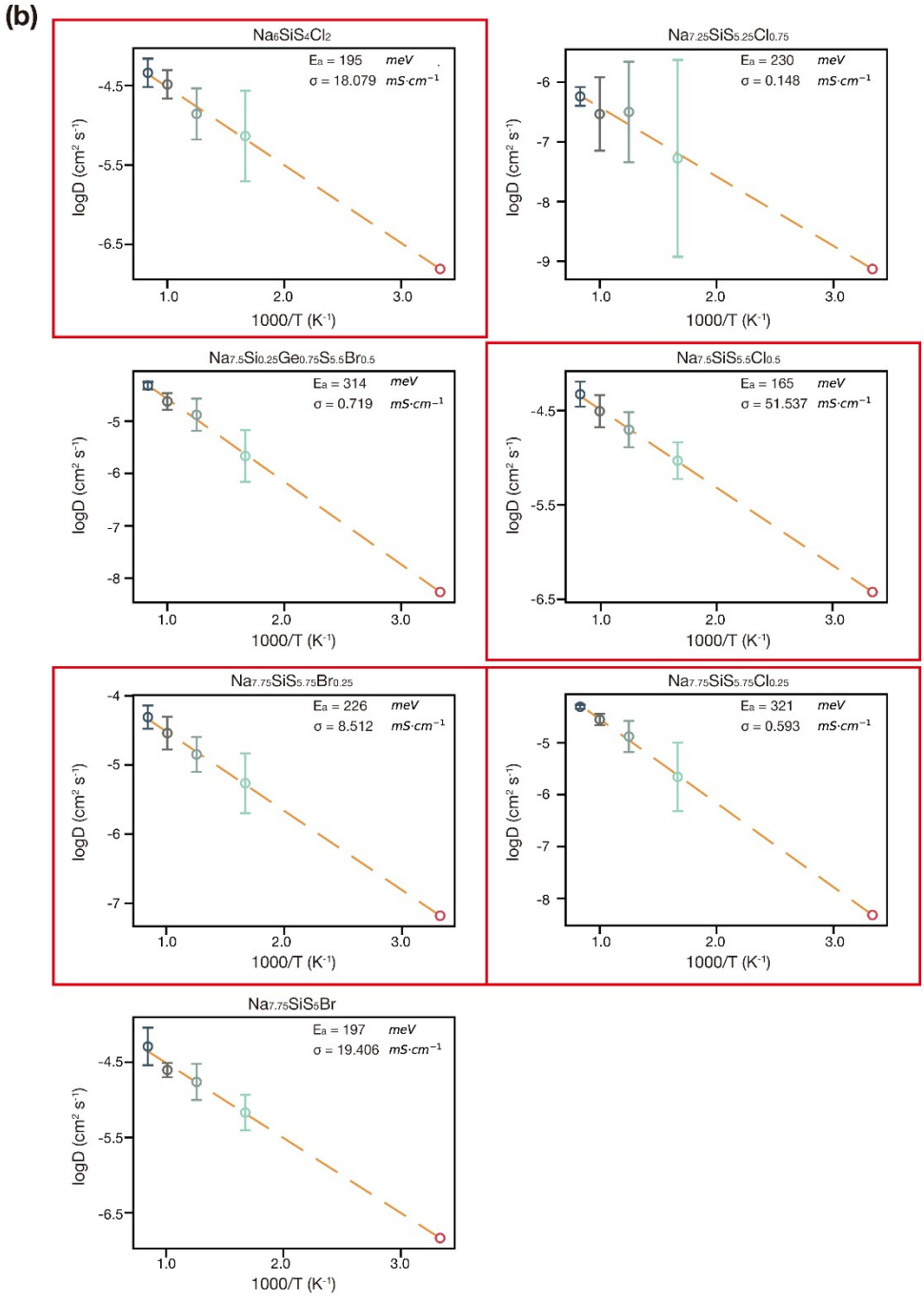

Fig. S4 (b). σ^{S}_{RT} results.

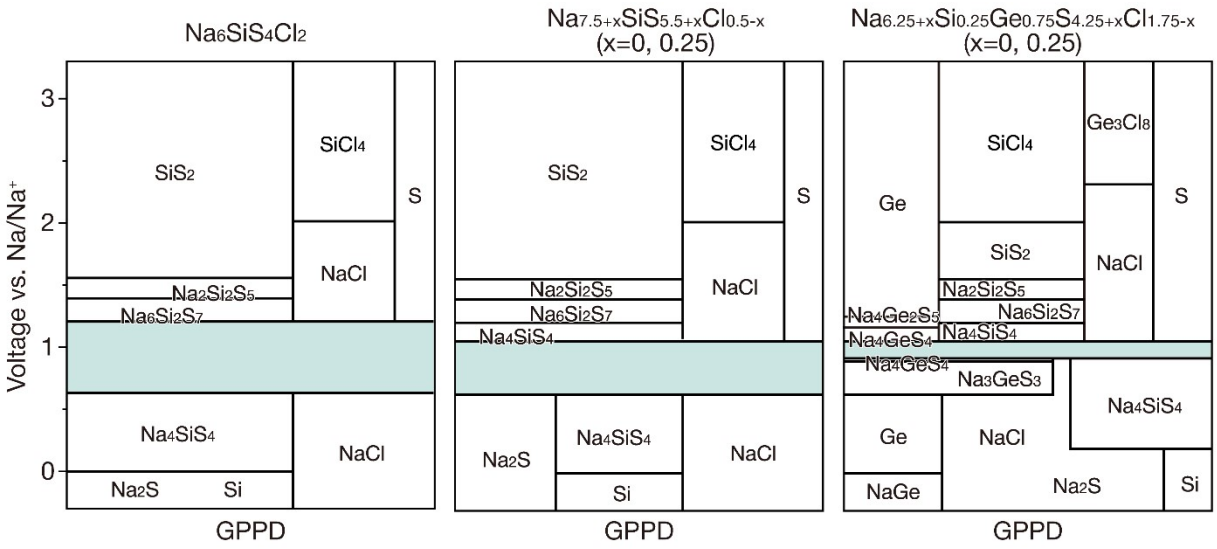

Supplementary Figure 5. Grand potential phase diagrams elucidating the phase equilibria and chemical reaction during oxidation and reduction process with respect to the Na chemical potential. The voltage stability window highlighted in yellow colour. These diagrams are just a more detailed and clearer view of those in Figure 4 in the manuscript.

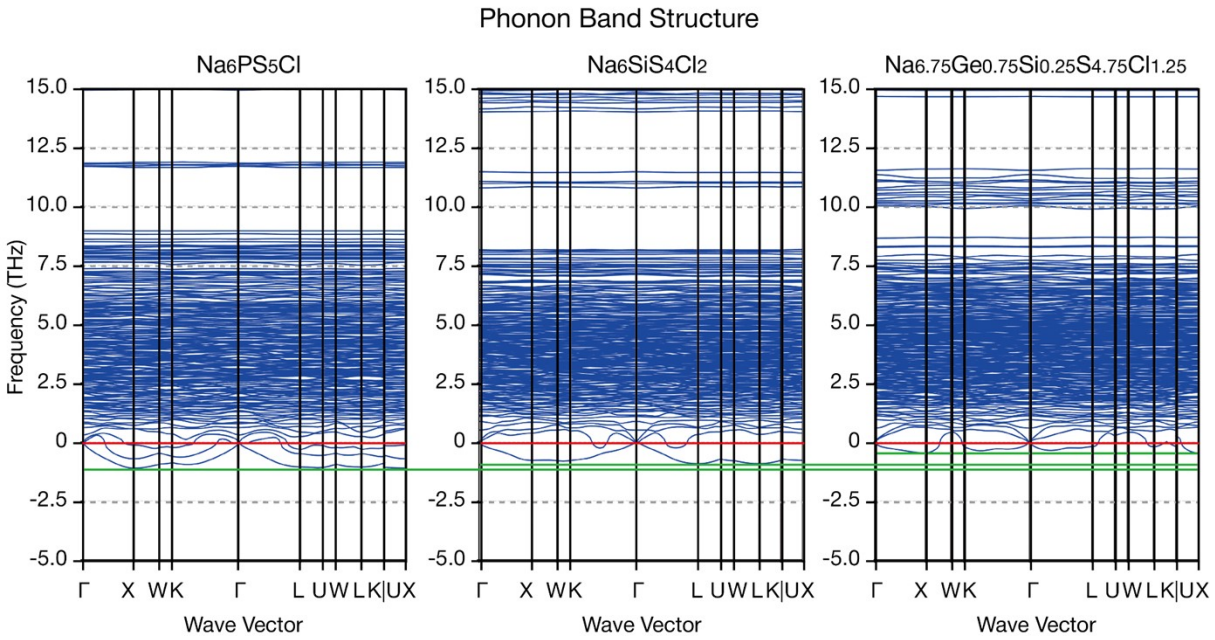

Supplementary Figure 6. Computed phonon dispersion curves for Na_6PS_5Cl, $Na_6SiS_4Cl_2$, and $Na_{6.75}Ge_{0.75}Si_{0.25}S_{4.75}Cl_{1.25}$ along high-symmetry directions in the Brillouin zone. While all structures exhibit imaginary frequencies indicating dynamical instabilities, the mixed-composition system $Na_{6.75}Ge_{0.75}Si_{0.25}S_{4.75}Cl_{1.25}$ shows reduced instability as evidenced by smaller magnitudes of imaginary frequencies (refer to green lines). The zero-frequency reference is marked by a red line.

Table S1. Detailed architectures and hyperparameters of the coGN and coNGN models. The model hyperparameters are adjusted to the values specified in the Matbench[1] configuration file, while remaining within the default values[2].

Component	Details	Shape
Model Inputs	**offset**	(Batch, 3)
	atomic_number	(Batch,)
	multiplicity	(Batch,)
	edge_indices	(Batch, 2)
Model Block	**Model Hyperparameters**	**Value**
Input Block	**Node Size:**	128
	Edge Size:	128
	Node embedding settings:	
	Atomic Mass	Included
	Atomic Radius	Included
	Electronegativity	Included
	Ionization Energy	Included
	Oxidation States	Included
	Edge Embedding Settings:	
	Number of Distance Bins	32
	Maximum Distance	8
	Distance Log Base	1
Processing Blocks/Nested Blocks (Repeated 5 times)	**Edge MLP:**	
	Units	[128, 128, 128, 128, 128]
	Activation	['swish', 'swish', 'swish', 'swish', 'swish']
	Node MLP:	
	Units	[128]
	Activation	['swish']
	Edge Attention MLP:	
	Units	[32, 1]
	Activation	['swish', 'swish']
	Edge Attention MLP (Global):	
	Units	[32, 1]
	Activation	['swish', 'swish']
	Node Attention MLP:	
	Units	[32, 1]
	Activation	['swish', 'swish']
	Aggregation Methods:	
	Edges (Local)	sum
	Return Updated:	
	Nodes	TRUE
	Globals	TRUE
	Residual Connections:	
	Node Update	TRUE
	Update Inputs Configuration:	
	Edges	[True, True, True, False]
	Nodes	[True, False, False]
	Globals	[False, True, False]

Table S1. Continued.

Model Block	Model Hyperparameters	Value
	Global MLP:	
	Units	[1]
	Activation	['linear']
	Attention MLP Settings:	
	Edge (Local) Units	[32, 1]
	Activation	['swish', 'swish']
	Edge (Global) Units	[32, 1]
	Activation	['swish', 'swish']
Output Block	Node Units	[32, 1]
	Activation	['swish', 'swish']
	Aggregation Methods:	
	Edges (Local)	sum
	Nodes	mean
	Return Updated:	
	Node	TRUE
	Globals	TRUE
	Multiplicity Readout:	TRUE

Table S2. All the electrolyte decomposition reactions for the five nominated Na-based argyrodites electrolytes.

$Na_6SiS_4Cl_2$

Potential ref to Na/Na+ (V)	Phase equilibria at the potential
0.00	4 $Na_6SiS_4Cl_2$ + 16 Na -> 16 Na_2S + 4 Si + 8 NaCl
0.63	4 $Na_6SiS_4Cl_2$ -> 4 Na_4SiS_4 + 8 NaCl
1.21	4 $Na_6SiS_4Cl_2$ -> 2 $Na_6Si_2S_7$ + 2 S + 8 NaCl + 4 Na
1.39	4 $Na_6SiS_4Cl_2$ -> 2 $Na_2Si_2S_5$ + 6 S + 8 NaCl + 12 Na
1.56	4 $Na_6SiS_4Cl_2$ -> 4 SiS_2 + 8 S + 8 NaCl + 16 Na
2.01	4 $Na_6SiS_4Cl_2$ -> 2 SiS_2 + 2 $SiCl_4$ + 12 S + 24 Na

$Na_{7.75}SiS_{5.75}Cl_{0.25}$

Potential ref to Na/Na+ (V)	Phase equilibria at the potential
0.00	4 $Na_{7.75}SiS_{5.75}Cl_{0.25}$ + 16 Na -> 23 Na_2S + 4 Si + NaCl
0.63	4 $Na_{7.75}SiS_{5.75}Cl_{0.25}$ -> 4 Na_4SiS_4 + 7 Na_2S + NaCl
1.06	4 $Na_{7.75}SiS_{5.75}Cl_{0.25}$ -> 4 Na_4SiS_4 + 7 S + NaCl + 14 Na
1.21	4 $Na_{7.75}SiS_{5.75}Cl_{0.25}$ -> 2 $Na_6Si_2S_7$ + 9 S + NaCl + 18 Na
1.39	4 $Na_{7.75}SiS_{5.75}Cl_{0.25}$ -> 2 $Na_2Si_2S_5$ + 13 S + NaCl + 26 Na
1.56	4 $Na_{7.75}SiS_{5.75}Cl_{0.25}$ -> 4 SiS_2 + 15 S + NaCl + 30 Na
2.01	4 $Na_{7.75}SiS_{5.75}Cl_{0.25}$ -> 3.75 SiS_2 + 0.25 $SiCl_4$ + 15.5 S + 31 Na

$Na_{7.5}SiS_{5.5}Cl_{0.5}$

Potential ref to Na/Na+ (V)	Phase equilibria at the potential
0.00	4 $Na_{7.5}SiS_{5.5}Cl_{0.5}$ + 16 Na -> 23 Na_2S + 4 Si + NaCl
0.63	4 $Na_{7.5}SiS_{5.5}Cl_{0.5}$ -> 4 Na_4SiS_4 + 7 Na_2S + NaCl
1.06	4 $Na_{7.5}SiS_{5.5}Cl_{0.5}$ -> 4 Na_4SiS_4 + 7 S + NaCl + 14 Na
1.21	4 $Na_{7.5}SiS_{5.5}Cl_{0.5}$ -> 2 $Na_6Si_2S_7$ + 9 S + NaCl + 18 Na
1.39	4 $Na_{7.5}S_1S_{5.5}Cl_{0.5}$ -> 2 $Na_2Si_2S_5$ + 13 S + NaCl + 26 Na
1.56	4 $Na_{7.5}SiS_{5.5}Cl_{0.5}$ -> 4 SiS_2 + 15 S + NaCl + 30 Na
2.01	4 $Na_{7.5}SiS_{5.5}Cl_{0.5}$ -> 3.75 SiS_2 + 0.25 $SiCl_4$ + 15.5 S + 31 Na

$Na_{6.75}Si_{0.25}Ge_{0.75}S_{4.75}Cl_{1.25}$

Potential ref to Na/Na+ (V)	Phase equilibria at the potential
0.00	4 $Na_{6.75}Si_{0.25}Ge_{0.75}S_{4.75}Cl_{1.25}$ + 19 Na -> 3 NaGe + 17 Na_2S + 7 NaCl + Si
0.20	4 $Na_{6.75}Si_{0.25}Ge_{0.75}S_{4.75}Cl_{1.25}$ + 16 Na -> 17 Na_2S + 7 NaCl + 3 Ge + Si
0.63	4 $Na_{6.75}Si_{0.25}Ge_{0.75}S_{4.75}Cl_{1.25}$ + 12 Na -> Na_4SiS_4 + 13 Na_2S + 7 NaCl + 3 Ge
0.90	4 $Na_{6.75}Si_{0.25}Ge_{0.75}S_{4.75}Cl_{1.25}$ + 3 Na -> 3 Na_3GeS_3 + Na_4SiS_4 + 4 Na_2S + 7 NaCl
0.92	4 $Na_{6.75}Si_{0.25}Ge_{0.75}S_{4.75}Cl_{1.25}$ -> 3 Na_4GeS_4 + Na_4SiS_4 + Na_2S + 7 NaCl
1.06	4 $Na_{6.75}Si_{0.25}Ge_{0.75}S_{4.75}Cl_{1.25}$ -> 3 Na_4GeS_4 + Na_4SiS_4 + 7 NaCl + S + 2 Na
1.17	4 $Na_{6.75}Si_{0.25}Ge_{0.75}S_{4.75}Cl_{1.25}$ -> Na_4SiS_4 + 1.5 $Na_4Ge_2S_5$ + 7 NaCl + 5.5 S + 8 Na
1.21	4 $Na_{6.75}Si_{0.25}Ge_{0.75}S_{4.75}Cl_{1.25}$ -> 0.5 $Na_6Si_2S_7$ + 1.5 $Na_4Ge_2S_5$ + 7 NaCl + 6 S + 9 Na
1.26	4 $Na_{6.75}Si_{0.25}Ge_{0.75}S_{4.75}Cl_{1.25}$ -> 0.5 $Na_6Si_2S_7$ + 7 NaCl + 13.5 S + 3 Ge + 15 Na
1.39	4 $Na_{6.75}Si_{0.25}Ge_{0.75}S_{4.75}Cl_{1.25}$ -> 0.5 $Na_2Si_2S_5$ + 7 NaCl + 14.5 S + 3 Ge + 17 Na
1.56	4 $Na_{6.75}Si_{0.25}Ge_{0.75}S_{4.75}Cl_{1.25}$ -> SiS_2 + 7 NaCl + 15 S + 3 Ge + 18 Na
2.01	4 $Na_{6.75}Si_{0.25}Ge_{0.75}S_{4.75}Cl_{1.25}$ -> $SiCl_4$ + 3 NaCl + 17 S + 3 Ge + 22 Na
2.31	4 $Na_{6.75}Si_{0.25}Ge_{0.75}S_{4.75}Cl_{1.25}$ -> $SiCl_4$ + 0.375 Ge_3Cl_8 + 17 S + 1.875 Ge + 25 Na

$Na_{6.25}Si_{0.25}Ge_{0.75}S_{4.25}Cl_{1.75}$

Potential ref to Na/Na+ (V)	Phase equilibria at the potential
0.00	4 $Na_{6.25}Si_{0.25}Ge_{0.75}S_{4.25}Cl_{1.75}$ + 19 Na -> 3 NaGe + 17 Na_2S + 7 NaCl + Si
0.20	4 $Na_{6.25}Si_{0.25}Ge_{0.75}S_{4.25}Cl_{1.75}$ + 16 Na -> 17 Na_2S + 7 NaCl + 3 Ge + Si
0.63	4 $Na_{6.25}Si_{0.25}Ge_{0.75}S_{4.25}Cl_{1.75}$ + 12 Na -> Na_4SiS_4 + 13 Na_2S + 7 NaCl + 3 Ge
0.90	4 $Na_{6.25}Si_{0.25}Ge_{0.75}S_{4.25}Cl_{1.75}$ + 3 Na -> 3 Na_3GeS_3 + Na_4SiS_4 + 4 Na_2S + 7 NaCl
0.92	4 $Na_{6.25}Si_{0.25}Ge_{0.75}S_{4.25}Cl_{1.75}$ -> 3 Na_4GeS_4 + Na_4SiS_4 + Na_2S + 7 NaCl
1.06	4 $Na_{6.25}Si_{0.25}Ge_{0.75}S_{4.25}Cl_{1.75}$ -> 3 Na_4GeS_4 + Na_4SiS_4 + 7 NaCl + S + 2 Na
1.17	4 $Na_{6.25}Si_{0.25}Ge_{0.75}S_{4.25}Cl_{1.75}$ -> Na_4SiS_4 + 1.5 $Na_4Ge_2S_5$ + 7 NaCl + 5.5 S + 8 Na
1.21	4 $Na_{6.25}Si_{0.25}Ge_{0.75}S_{4.25}Cl_{1.75}$ -> 0.5 $Na_6Si_2S_7$ + 1.5 $Na_4Ge_2S_5$ + 7 NaCl + 6 S + 9 Na
1.26	4 $Na_{6.25}Si_{0.25}Ge_{0.75}S_{4.25}Cl_{1.75}$ -> 0.5 $Na_6Si_2S_7$ + 7 NaCl + 13.5 S + 3 Ge + 15 Na
1.39	4 $Na_{6.25}Si_{0.25}Ge_{0.75}S_{4.25}Cl_{1.75}$ -> 0.5 $Na_2Si_2S_5$ + 7 NaCl + 14.5 S + 3 Ge + 17 Na
1.56	4 $Na_{6.25}Si_{0.25}Ge_{0.75}S_{4.25}Cl_{1.75}$ -> SiS_2 + 7 NaCl + 15 S + 3 Ge + 18 Na
2.01	4 $Na_{6.25}Si_{0.25}Ge_{0.75}S_{4.25}Cl_{1.75}$ -> $SiCl_4$ + 3 NaCl + 17 S + 3 Ge + 22 Na
2.31	4 $Na_{6.25}Si_{0.25}Ge_{0.75}S_{4.25}Cl_{1.75}$ -> $SiCl_4$ + 0.375 Ge_3Cl_8 + 17 S + 1.875 Ge + 25 Na

References

[1] Dunn, A.; Wang, Q.; Ganose, A.; Dopp, D.; Jain, A. Benchmarking Materials Property Prediction Methods: The Matbench Test Set and Automatminer Reference Algorithm. *npj Comput. Mater.* **2020**, *6* (1), 138. https://doi.org/10.1038/s41524-020-00406-3.

[2] Ruff, R.; Reiser, P.; Stühmer, J.; Friederich, P. Connectivity Optimized Nested Graph Networks for Crystal Structures. *Digit. Discov.* **2024**, 3, 594-601. https://doi.org/10.1039/D4DD00018H

[3] Choudhary, K.; DeCost, B. (2021). Atomistic Line Graph Neural Network for improved materials property predictions. *npj Comput. Mater.* **2021***, 7*(1), 185. https://doi.org/10.1038/s41524-021-00650-1

[4] Schütt, K. T.; Kindermans, P. J.; Sauceda, H. E.; Chmiela, S.; Tkatchenko, A.; Müller, K. R. SchNet: A continuous-filter convolutional neural network for modeling quantum interactions. *Advances in Neural Information Processing Systems*, *2017-December*, 992–1002.

[5] Klicpera, J.; Giri, S.; Margraf, J. T.; Gunnemann, S. Fast and Uncertainty-Aware Directional Message Passing for Non-Equilibrium Molecules. *arXiv* DOI: 10.48550/arXiv.2011.14115 (accessed 2022-04-05).

[6] Cheng, G.; Gong, X.-G.; Yin, W.-J. Crystal structure prediction by combining graph network and optimization algorithm. *Nat. Commun.* **2022**, *13*(1), 1492. https://doi.org/10.1038/s41467-022-29241-4.

[7] Chen, C.; Ye, W.; Zuo, Y.; Zheng, C.; Ong, S. P. Graph Networks as a Universal Machine Learning Framework for Molecules and Crystals. *Chem. Mater.* **2019**, *31*(9), 3564–3572. https://doi.org/10.1021/acs.chemmater.9b01294.

[8] Xie, T.; Grossman, J. C. Crystal Graph Convolutional Neural Networks for an Accurate and Interpretable Prediction of Material Properties. *Phys. Rev. Lett.* **2018**, *120*(14), 145301. https://doi.org/10.1103/PhysRevLett.120.145301

[9] Ihalage, A.; Hao, Y. Formula Graph Self-Attention Network for Representation-Domain Independent Materials Discovery. *Adv. Sci.* **2022** *9*(18), 2200164. https://doi.org/https://doi.org/10.1002/advs.202200164.

[10] De Breuck, P.-P.; Evans, M. L.; Rignanese, G.-M. Robust model benchmarking and bias-imbalance in data-driven materials science: a case study on MODNet. *J. Phys. Condens. Matter.* **2021**, *33*(40), 404002. https://doi.org/10.1088/1361-648X/ac1280.

[11] Wang, A. Y.-T.; Kauwe, S. K.; Murdock, R. J.; Sparks, T. D. Compositionally restricted attention-based network for materials property predictions. *npj Comput. Mater.* **2021** *7*(1), 77. https://doi.org/10.1038/s41524-021-00545-1.

[12] Chen, T.; Guestrin, C. XGBoost: A Scalable Tree Boosting System. *Proceedings of the 22nd ACM SIGKDD International Conference on Knowledge Discovery and Data Mining*, 2016 785–794. https://doi.org/10.1145/2939672.2939785.